Controlling surface properties of electrospun polyphenylsulfone using plasma treatment and X-ray photoelectron spectroscopy

Kion Norrman [c,*], Yan Wang [b], Eugen Stamate [a], Wenjing Zhang [a,**]

[a] Department of Energy Conversion and Storage, Technical University of Denmark, Frederiksborgvej 399, DK-4000, Roskilde, Denmark
[b] Department of Chemical Engineering, Huaihai Institution of Technology, 222005, Lianyungang City, People's Republic of China
[c] Center for Integrative Petroleum Research, King Fahd University of Petroleum & Minerals, KFUPM Box 5070, Dhahran 31261, Saudi Arabia

ARTICLE INFO

ABSTRACT

Plasma treatment is an efficient method to modify organic surfaces. In this work electrospun polyphenylsulfone was systematically subjected to low-pressure microwave plasma and atmospheric-pressure coplanar barrier discharge in order to control the surface chemistry, which is important for controlling surface properties. Polar anchor groups such as keto/aldehyde groups and especially carboxylic acid groups affect hydrophilicity. The composition of plasma-induced chemical anchor groups can be monitored (and thus controlled) by X-ray photoelectron spectroscopy. The atmospheric-pressure plasma provided subtle oxidation, and the low-pressure plasma provided significant oxidation that resulted in polyphenylsulfone surfaces with a very high hydrophilicity. The low-pressure plasma treated polyphenylsulfone exhibited a significant age effect over 212 days, which was attributed to a diffusion phenomenon where the polyphenylsulfone surface becomes enriched in non-oxidated polyphenylsulfone. It was shown that the improved hydrophilicity will diminish but not vanish in time.

1. Introduction

The discovery of electrospun nanofiber materials has resulted in a broad spectrum of useful applications within heterogeneous catalysis, water purification, air filtration, energy conversion/harvesting/storage, smart textiles, tissue engineering, regenerative medicine, sensors for biological sensing, and drug delivery [1, 2, 3, 4, 5, 6, 7, 8, 9, 10, 11, 12, 13, 14, 15, 16]. Depending on the application various properties need to be carefully controlled, e.g. composition, structure, porosity, and surface properties.

The current work focuses on controlling the hydrophilicity of electrospun nanofibrous (i.e. non-woven) membrane surfaces used within water purification. Hydrophilicity is an important parameter for controlling the wettability of the membrane. Electrospinning produces membranes that are very versatile, simple, and efficient when it comes to water purification [7, 8, 9, 10]. Typically employed electrospun membranes within water purification are polyvinyl chloride, polyvinylidene fluoride, polysulfone, polyvinyl alcohol, polyacrylonitrile, polyurethane, and cellulose acetate [17, 18, 19, 20, 21, 22]. Electrospun nanofibrous membranes have advantageous properties, such as high porosity, large flexibility in pore sizes, high permeability, interconnected open pore structure, and large surface to volume ratios, which is useful for controlling surface properties via surface modification. One of the most efficient methods to improve the integrity and the mechanical strength of electrospun nanofibrous membranes is heat treatment above the glass transition temperature that will fuse the fibers together at the junction points [21, 22, 23, 24]. Membrane materials used for water purification/filtration have to be hydrophilic, which is an important issue for the wettability of membranes. An improved wettability will significantly reduce the capillary pressure of the membrane and increase the flow rate of the liquid. Hydrophilicity will impede biofouling and clogging (adsorption of protein and bacteria) of the membrane during the water purification process [19]. However, the most commonly used membrane materials within water purification are hydrophobic, e.g. polyvinylidene fluoride (PVDF), polytetrafluoroethylene (PTFE), polypropylene (PP), and polyethersulfone (PES). Various methods can be used to modify hydrophobic membrane surfaces into hydrophilic membrane surfaces, such as blending with hydrophilic polymers [25, 26, 27], chemical oxidation and grafting [28], and plasma treatment [29].

Polyphenylsulfone (PPSU), polysulfone (PSU), and PES belongs to the group of polymers that has an aromatic backbone including an ether and a sulfone unit as part of the backbone. This group of polymers exhibit

---

superior properties in terms of thermal stability, chemical resistance, and impact resistance [30, 31, 32]. Preliminary results from our lab suggest that PPSU has better membrane properties compared to PES and PSU, so the current work is focused exclusively on this polymer. The authors Gonzales et al. [33]. employed low-temperature atmospheric-pressure oxygen plasma on the before mentioned group of polymers in order to study the effect of plasma on the molecular structures of the polymers. In the current work electrospun PPSU nanofibrous membranes were treated with two different types of plasma, based on (i) low-pressure microwave plasma, and (ii) atmospheric-pressure coplanar barrier discharge. The current work focuses on attempting to control the surface chemistry in order to optimize hydrophilicity (and thus wettability) by systematically exposing electrospun PPSU membrane surfaces to plasma. The surface chemistry is monitored by X-ray photoelectron spectroscopy (XPS). The results are reported herein. The work described in this paper is part of larger project where other aspects of the PPSU membranes are described, such as morphology, contact angle, mechanical and separation properties [34].

2. Materials and methods

2.1. Materials, fabrication, and post heat treatment

The PPSU polymer Radel® R-5500NT was obtained from Solvay Advanced Polymer LLC. The solvents N-methyl-2-pyrrolidone (NMP) and acetone were supplied from Sigma-Aldrich. All materials were used as received. PPSU was dissolved in a binary solvent system of NMP/acetone with a 8:2 weight ratio by stirring at room temperature for 24 hours in order to obtain a homogenous 30 wt% solution. Membranes were prepared by employing an electrospinning apparatus purchased from Linari Nanotech. The polymer solutions were transferred into a 10 ml plastic syringe and squeezed out through a metal needle with an inner diameter of 0.8 mm at a constant flow rate of 0.2 ml per hour. The positive electrode of the high voltage power supply was connected to the metal needle. The grounded electrode was connected to a stainless steel drum wrapped with silicon coated kraft paper and rotated at 100 rpm. During the electrospinning the applied voltage and the collecting distance were 15 kV and 12 cm, respectively. The relative humidity and temperature were kept at 19–22% and 29–30 °C, respectively. The as-spun membranes were post-heat treated in oven at 240 °C for one hour to improve the mechanical properties of the membranes. The sides of the membrane were fixed during heat treatment in order to prevent shrinkage.

2.2. Plasma treatment

Various plasma sources can be used to produce reactive species able to modify the surface properties of materials, including tuning of hydrophilicity [35, 36]. O_2 gas can be dissociated in low-pressure discharges to produce atomic oxygen. At the same time, atmospheric-pressure discharges operated in air or O_2 can additionally produce highly reactive O_3. For improving the wettability of PPSU membranes, two different methods were employed, (i) low-pressure microwave plasma and (ii) atmospheric-pressure coplanar barrier discharge. While microwave plasma can provide a very well controlled environment suitable for tuning the surface chemistry, which can be carefully monitored using XPS analysis, the atmospheric plasma was chosen as test for a low cost and high throughput alternative.

2.3. Low-pressure microwave plasma

The discharge was produced in a cubical vacuum chamber of $40 \times 40 \times 40$ cm^3, equipped with 12 electron cyclotron resonance (ECR) plasma cells [37] powered by microwaves at 2.45 GHz. A more detailed description is presented elsewhere [38]. The magnetic filter used to reduce the electron temperature was removed for this set of experiments. The O_2 dissociation rate was evaluated using a HIDEN mass spectrometer

and plasma parameters (electron temperature, T_e, plasma density, n_e, and plasma potential, V_{pl}) were measured by a spherical Langmuir probe [39] made of platinum, at the same location used to treat the PPSU membrane. O_2 dissociation needs a large fraction of energetic electrons so that the discharge pressure was set at 5 mTorr. The discharge power was adjusted to 500 and 1000 W, which corresponded to the plasma parameters listed in Table 1. The O_2 dissociation rate was 29% at 500 W and 33% at 1000 W, respectively. The 5×10 cm^2 membranes were placed, using a rectangular frame, at 15 cm below the ECR plasma cells, at the center of the vacuum chamber, and were exposed to plasma discharge for 1 or 2 minutes on each side. Since the chamber is rather large, one expects a direct treatment on the top side (exposed to the microwave plasma cells) and a reduced treatment on the lower side that faces a lower plasma density. By rotating the membrane after equal intervals of time, one expects the same integrated effect on the surface. Consequently, the membranes were exposed to a high concentration of atomic oxygen while the plasma heating was kept below 70 °C.

2.4. Atmospheric-pressure coplanar barrier discharge

The coplanar barrier discharge [40] is part of a larger category of atmospheric-pressure plasma sources, defined as dielectric barrier discharges. Due to their large potential for surface treatment of different materials, including glasses, polymers and textiles, as well as biomedical applications (bacterial inactivation) and gas phase chemistry (NOx and VOC reduction) a large variety of dielectric barrier discharges have been developed. Among them, the coplanar barrier discharge (sometime defined as surface barrier discharge) is particularly suited for treatment of flat surfaces in static or roll-to-roll processes. Besides many custom-made configurations, Kyocera® has recently introduced a multilayer ceramic technology, where imbricated electrodes are immersed into a ceramic dielectric barrier. Such a plasma source was recently evaluated in ozone production and NOx reduction [41] and was also available for the experiments reported in this work. Thus, the active plasma region of 40×50 mm^2 was placed 2.5 mm above the PPSU membrane, situated on a glass substrate. A Tantec® power supply operating in resonant mode at 23 kHz was used to power the discharge at 100 W. The membranes were treated for 0.5, 1, and 3 minutes on each side with the purpose of testing the capability of improving the membranes wettability. No visible changes (coloring, deformation) were observed for samples treated at 0.5 and 1 minute while the sample treated for 3 minutes exhibited a slight brown coloring, so treatments longer than 3 minutes were not attempted.

2.5. XPS analysis

The XPS analyses were performed on a ESCALAB XI$^+$ X-ray photoelectron spectrometer microprobe (Thermo Fisher Scientific, East Grinstead, U.K.) using a monochromatic Al-Kα X-ray source with a 650 μm spot size and a take-off angle of 90° from the surface plane. Atomic concentrations were determined from survey spectra (0–1350 eV, 100 eV detector pass energy, 1 eV step size, 50 ms dwell time, 3 scans) and were calculated by determining the relevant integral peak intensities using a Smart type background. Five different surface locations were analyzed on each sample surface and average values were calculated. High-resolution C 1s, O 1s, and S 2p spectra were acquired (50 eV detector pass energy, 0.1 eV step size, 50 ms dwell time, 5–20 scans) and the Thermo Fisher Scientific Avantage software (version 5.979, build 06465) was employed for peak fitting, using a Smart type background, a full width at half maximum (FWHM) of 1.5 eV, and a Gauss/Lorentz mix value of 35%. The spectrometer was calibrated using the peaks Au 4f7 (84.0 eV), Ag 3d5 (368.3 eV), and Cu 2p3 (932.8 eV), which is in excellent agreement with the average National Institute of Standards and Technology (NIST) values: Au 4f7 (84.0 ± 0.1 eV), Ag 3d5 (368.2 ± 0.1 eV), and Cu 2p3 (932.6 ± 0.2 eV) [42].

Table 1

Plasma parameters used to treat the PSSU membranes.

Plasma type	Pressure [Torr]	Power [W]	Time [min.]	Density [m^{-3}]	Electron temp. [eV]	Plasma potential [V]
Microwave	5×10^{-3}	1000	2 + 2	9.7×10^{15}	0.9	8.3
Microwave	5×10^{-3}	1000	1 + 1	9.7×10^{15}	0.9	8.3
Microwave	5×10^{-3}	500	1 + 1	6.6×10^{15}	0.7	8.1
Microwave	5×10^{-3}	500	2 + 2	6.6×10^{15}	0.7	8.1
Dielectric	760	100	0.5 + 0.5	–	–	–
Dielectric	760	100	1 + 1	–	–	–
Dielectric	760	100	3 + 3	–	–	–

3. Results and discussion

3.1. Effect of discharge power and exposure time

PPSU membrane samples were systematically subjected to low-pressure or atmospheric-pressure plasma treatment. SEM images before and after plasma treatment revealed that plasma treatment induced no significant morphological changes of the porous network [34]. Plasma parameters are listed in Table 1, and XPS acquired element compositions are listed in Table 2. Low-pressure plasma (microwave) properties are more easily controllable, and thus the better choice for tuning surface chemistry and thus hydrophilicity/wettability. However, atmospheric-pressure plasma (dielectric) is a low cost non-vacuum technique with a high throughput, so it is obvious to consider it as an alternative to low-pressure plasma.

During the plasma process oxygen is activated and reacts with the PPSU membrane surface causing oxidation of the PPSU polymer chains, i.e. oxygen is added to the molecular structure. Gonzalez et al. [33] suggested that the aromatic rings react with plasma induced activated oxygen atoms that results in molecular ring opening and oxidation producing equal amounts of aldehyde and carboxylic acid groups without chain scission. The ring opening process sounds intuitively realistic, but it only describes one of many possible reactions occurring during the plasma process. A more realistic picture is a distribution of reactions, where one or more reactions could dominate. Overall it is a complex situation where the complexity undoubtable increases with increasing power/dose up until the reaction products becomes gaseous combustion products. However, plasma parameters are typically tuned such that degradation is limited, which will enable some degree of control of the surface chemistry.

Earlier work [43, 44] from this lab on photooxidation of PES clearly demonstrates the complexity of the oxidation process. It was found that cross-linking was an important process during photoirradiation in vacuum. In ambient air at 1000 mbar oxygen reacts quickly with PES during photoirradiation, and chain scission was found to be the dominant process, and oxygen incorporation was found to be non-specific but pronounced for –SO$_3$H group formation. However, it should be emphasized that photo-induced oxidation do not necessarily results in the same reactions, and thus reaction products, as plasma-induced oxidation.

From the element compositions listed in Table 2 a lot of useful comparisons are possible. If the degree of oxidation is considered, then it is clear that the atmospheric-plasma is much less harsh compared to low-pressure plasma under the experimental conditions in question. The PPSU sample that was atmospheric-plasma treated for only 1 minute was oxidated to a degree that is less than the uncertainty when the reference is considered. However, after 2 minutes the oxidation becomes detectable, and after 6 minutes the oxidation becomes significant (~5.5 atom% increase in oxygen), but still subtle compared to the weakest treatment using low-pressure plasma (~20 atom% increase in oxygen). The relative oxygen values for low-pressure plasma show that doubling the power from 500 to 1000 W for 2 minutes exposure time, only increases the oxygen content by ~1 atom%, but doubling the time from 2 to 4 minutes at 500 W, increases the oxygen content by ~2 atom%, and ~5 atom% at 1000 W. The power versus exposure time effect can be explained from the fact that doubling the power does not double the plasma density (Table 1), so exposure time is expected to be the most suitable tuning parameter.

The carbon values in Table 2 are obviously affected by the oxygen uptake, i.e. when the oxygen content increases then the carbon content will be relatively smaller. However, this should also be true for the sulfur content, but that is not observed, instead the sulfur content is observed to be either the same or a little bit less or more compared to the reference value. No explanation has been found for this observation.

High-resolution C 1s XPS spectra were acquired for all samples and deconvoluted into sub-peaks representing various carbon functionalities (Fig. 1). Fig. 1a explains the origin of the various native peaks (C=C, C–S, C–O). PPSU do not contain any native aliphatic carbon (C–C) in the molecular structure (Fig. 1a), but the peak (labeled "b") is present. This is due to adventitiously adsorbed hydrocarbons from ambient air. It is unfortunately unavoidable and it remains on the sample surfaces in the XPS vacuum chamber during analysis and in the plasma chamber, which complicates the experiments. However, since the adsorbed hydrocarbons are presumably small molecules, the plasma process will most likely produce oxidation products that are so small that they will evaporate. However, moving the samples from the plasma chamber to the XPS chamber result in further adsorption of hydrocarbons, a process that takes place within seconds. The C–C peak in the C 1s XPS spectrum in Fig. 1b (i.e. spectrum of reference sample) is most likely only adsorbed hydrocarbons. However, it becomes a bit more complicated for the plasma treated PPSU samples, because they will contain adsorbed hydrocarbons (i.e. C–C), but there could also be a contribution from plasma induced degradation of the aromatic carbon in PPSU that could produce aliphatic carbon (C–C).

Table 3 shows the distribution of carbon functionalities for selected plasma treatment conditions. There is a small C=O peak (0.5%) in the spectrum for the reference sample (0 W, 0 min), which should not be there, and the C–O/C–S ratio is a little smaller than expected, suggesting that some of the C–O had somehow oxidated to C=O between membrane

Table 2

XPS acquired element compositions for non-aged PPSU membranes at various plasma treatment conditions.

Element	Reference	Low-pressure plasma				Atmospheric-pressure plasma		
	0 W	500 W	500 W	1000 W	1000 W	100 W	100 W	100 W
	0 min. [atom%][a]	2 min. [atom%]	4 min. [atom%]	2 min. [atom%]	4 min. [atom%]	1 min. [atom%]	2 min. [atom%]	6 min. [atom%]
C	81.0 ± 0.4	60.8 ± 0.1	58.1 ± 0.2	60.1 ± 0.3	53.5 ± 0.5	80.8 ± 0.1	80.1 ± 0.3	74.7 ± 0.8
O	14.9 ± 0.3	35.1 ± 0.1	37.2 ± 0.2	36.2 ± 0.3	41.6 ± 0.5	15.2 ± 0.1	16.1 ± 0.2	21.5 ± 0.8
S	4.2 ± 0.1	4.1 ± 0.1	4.7 ± 0.1	3.7 ± 0.1	5.0 ± 0.1	4.0 ± 0.1	3.8 ± 0.1	3.8 ± 0.1

[a] All values are averages based on five measurements on different surface locations.
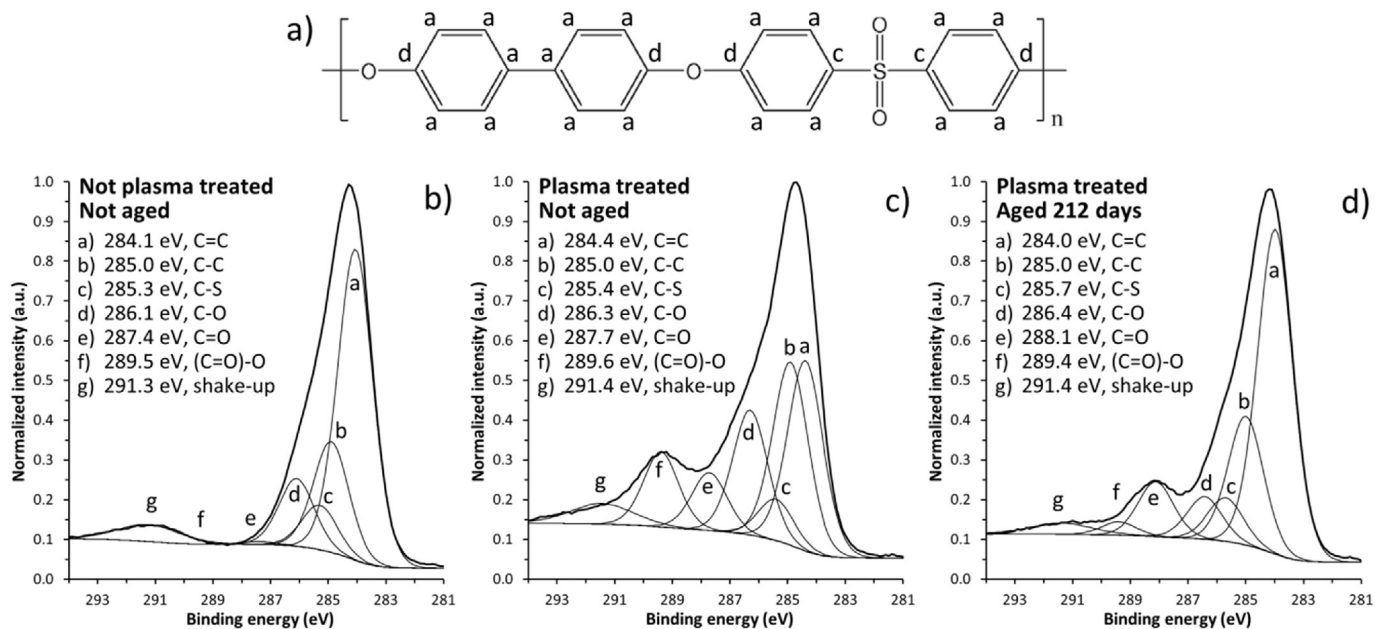
Fig. 1. High-resolution C 1s XPS spectra of a PPSU membranes (a) that was neither plasma treated or aged (b), a low-pressure plasma treated (1000 W, 4 min) membrane that was not aged (c), and a membrane that was plasma treated (1000 W, 4 min) and aged for 212 days (d).

Table 3
Quantification of selected deconvoluted C 1s spectra for non-aged PPSU membranes for various plasma treatment conditions.

| Denconv. peak	0 W 0 min [%]	100 W[a] 6 min [%]	500 W[b] 2 min [%]	500 W[b] 4 min [%]	1000 W[b] 2 min [%]	1000 W[b] 4 min [%]
C=C	57.9	50.6	30.9	30.7	30.6	28.3
C–C	20.7	20.1	19.1	21.3	24.5	27.2
C–S	8.3	7.9	8.0	7.4	7.4	6.1
C–O	12.6	14.8	22.2	20.1	18.8	18.6
C=O	0.5	4.2	10.6	10.7	9.1	8.6
(C=O)–O	0	2.3	9.2	9.8	9.5	11.2

[a] Atmospheric-pressure (760 Torr) plasma.
[b] Low-pressure (5×10^{-3} Torr) plasma.

fabrication and XPS analysis. Table 3 reveals a lot of details about the oxidation mechanisms. First of all the C=C, i.e. aromatic carbon, is observed to disappear for more harsh plasma conditions, which suggests that a molecular ring opening occurs during the plasma induced oxidation, consistent with the observations by Gonzalez et al. [33] Furthermore, the level of adventitiously adsorbed hydrocarbon on the PPSU membrane surfaces are expected to be the same, corresponding to the level on the reference sample (~20 atom%). However, at the two most harsh plasma conditions (2 and 4 min at 1000 W) the C–C content is observed to increase, suggesting that aliphatic carbon is formed subsequent to the ring opening. Just like the C=C functionality can either remain or disappear (i.e. not be formed), so can the C–S functionality (i.e. Ar–SO$_2$–Ar), it will either remain or undergo chain scission, it is highly unlikely that it will be formed during plasma oxidation. C–S is observed to decrease, but not by much, and it requires rather harsh plasma conditions, i.e. it requires harsh plasma conditions for PPSU to undergo chain scission at the C–S bond. The C–O functionality is complicated, it can disappear if chain scission occurs (i.e. at Ar-O-Ar → Ar-OH + ArH), but it can also be formed from hydroxyl formation (R–OH or Ar-OH, where R is aliphatic carbon and Ar is aromatic carbon), and it can be further oxidized to C=O, so there are competing reactions in play. However, there appears to be a maximum of C–O functionalities corresponding to 2 minutes of low-pressure plasma at 500 W. The C=O

functionality is also complicated since it is an intermediate oxidation product, i.e. C–OH → C=O → (C=O)–O. The maximal occurrence of C=O is observed for low-pressure plasma at 500 W. The (C=O)–O functionality is either in the form of a carboxylic acid or less likely an ester, and constitutes the end oxidation product. (C=O)–O is apparently readily formed even at low-pressure plasma at 500 W, but is then observed to only increase slightly (~2 atom%) for the most harsh plasma conditions (4 min at 1000 W), which is surprising. In terms of hydrophilicity/wettability the interesting functionalities are the more polar ones, which are C=O, (C=O)–O, and C-SO$_X$. However, both C=O and (C=O)–O are according to Table 3 efficiently formed at the weakest low-pressure plasma conditions (2 min at 500 W) that only changes slightly for harsher plasma conditions. This suggests that the wettability is expected to be more or less similar for all low-pressure plasma conditions. The results in Table 3 suggest that is possible, to some degree, to control the distribution of carbon functionalities. The harshest atmospheric-pressure plasma conditions appear to be an intermediate of no plasma and the weakest low-pressure plasma, which is practical when attempting to control the surface chemistry.

From the high-resolution S 2p XPS spectra in Fig. 2 it is evident that the sulfone group undergoes further oxidation resulting in the formation of –SO$_3$ and –SO$_4$ groups (–SO$_2$– → –SO$_3$ → –SO$_4$) with resulting chain scission of the polymer backbone. In the literature this process is typically described as only forming –SO$_4$ groups, which is intuitively surprising [23, 26]. However, in this work fitting using three 2p3/2p1 components gave the best fitting results. The S 2p XPS spectrum for the low-pressure plasma treated PPSU sample (Fig. 2b) reveals that approximately 50% of the sulfone groups have been further oxidized. However, there is a discrepancy relative to the C–S content listed in Table 3 for the same sample, that suggests an ~27% decrease compared to the reference sample (8.3%–6.1%). No explanation has been found for this discrepancy.

The effect of plasma power and exposure time on the distribution of sulfur functionalities is shown in Table 4. The –SO$_3$ functionality is an intermediate oxidation product that is observed to have a maximum occurrence at 2 min low-pressure plasma at 500 W. The –SO$_4$ functionality is an end oxidation product, and is observed to be readily formed even at the weakest plasma treatment and surprisingly stays at the same level until the harshest plasma conditions are reached where it increases
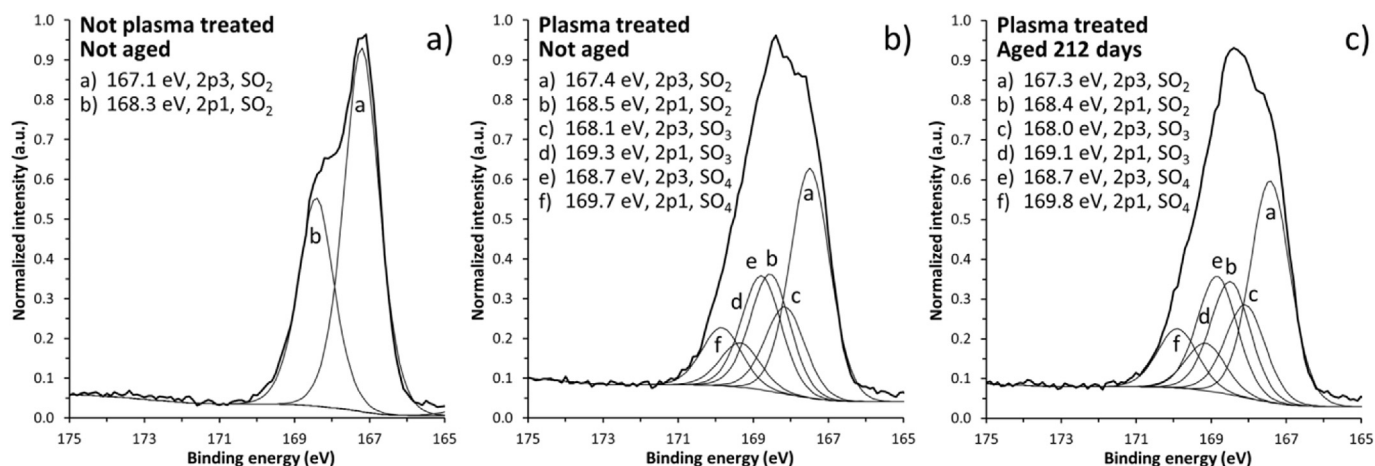
Fig. 2. High-resolution S 2p XPS spectra of a PPSU membranes that was neither plasma treated or aged (a), a low-pressure plasma treated (1000 W, 4 min) membrane that was not aged (b), and a membrane that was plasma treated (1000 W, 4 min) and aged for 212 days (c).

Table 4

Quantification of selected deconvoluted S 2p spectra for non-aged PPSU membranes for various plasma treatment conditions.

| Denconv. peak	0 W 0 min [%]	100 W[a] 1 min [%]	100 W[a] 6 min [%]	500 W[b] 2 min [%]	1000 W[b] 4 min [%]
$-SO_2-$	100.0	73.1	67.3	55.3	53.3
$-SO_3$	0.0	12.4	18.3	30.3	20.2
$-SO_4$	0.0	14.5	14.4	14.3	26.5

[a] Atmospheric-pressure (760 Torr) plasma.
[b] Low-pressure (5×10^{-3} Torr) plasma.

significantly. The results in Table 4 suggests that is possible to control at least the $-SO_3$ formation, whereas the formation of $-SO_4$ is more difficult to control. From a wettability point of view it is advantageous to have as many of $-SO_3$ and $-SO_4$ as possible.

Deconvoluting a high-resolution O 1s XPS spectrum from an organic sample surface that has been exposed to oxidative plasma treatment is challenging. In reality there are so many possible types of oxygen

functionalities formed that it becomes impossible to perform a fit that is even close to the real situation. The typical solution is to simplify the situation and only use a few components to the fitting procedure based on the assumed major components. For these types of systems two components have typically been used [30, 33]. In this work the least amount of components were used that produced the best fit possible. Fig. 3 displays the high-resolution O 1s XPS spectra for a reference PPSU sample and a plasma treated PPSU sample. In Fig. 3b the two native oxygen functionalities are shown in the expected 1:1 ration. A third unknown component at 535.0 eV is contributing to the overall O 1s peak. For the plasma treated PPSU sample (Fig. 3c) four components produced the best fit with the least amount of components. The unknown component at 535.0 eV is still present, but a new component "c" is now present at 533.5 eV. It is difficult to speculate further since there presumably will be a lot of peak overlap from various functionalities, e.g. it is known that the O 1s binding energy for $-SO_2-$ is the same as for C=O. It is clear that O 1s XPS spectra for plasma treated PPSU surfaces are not suited for monitoring detailed development of functionalities as a function of plasma conditions.
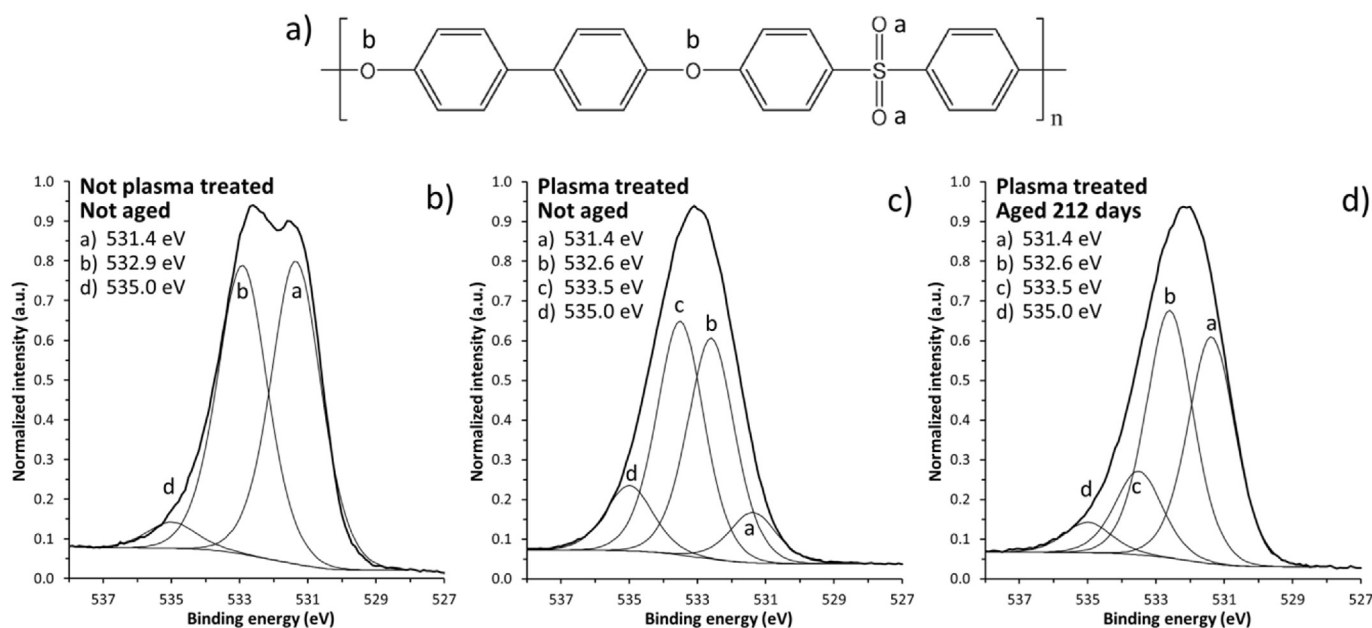
Fig. 3. High-resolution O 1s XPS spectra of a PPSU membranes (a) that was neither plasma treated or aged (b), a low-pressure plasma treated (1000 W, 4 min) membrane that was not aged (c), and a membrane that was plasma treated (1000 W, 4 min) and aged for 212 days (d).

3.2. Effect of ageing

The reference PPSU membrane and the low-pressure plasma treated (4 min at 1000 W) PPSU membrane were XPS analyzed in intervals over 212 days in order to map possible time effects. In between measurements the membrane samples were stored in darkness in ambient air at room temperature. The result is shown in Fig. 4. The composition plots versus time clearly exhibit an age effect.

The element composition for the plasma treated membrane remains unchanged for at least 168 hours (7 days) where after the measured oxygen content starts to decrease with the approximate same amount as the relative carbon content increases. The sulfur content is only slightly affected. This development is in progress even after 5088 hours (212 days). One possible explanation to the observed decrease of oxygen over time for the plasma treated PPSU membrane could be that hydrophilic anchor groups attached to the molecular structure, or fragments of, diffuse into the bulk, i.e. to non-plasma treated parts, which is plausible if the bulk is less hydrophobic compared to the PPSU/air interface. The plasma treatment has a limited penetration depth, which is, however, deeper than the probe depth (5–10 nm) of the XPS analysis. Since the plasma treatment depth is significantly larger than the XPS probe depth, it explains why no initial change is observed in the element composition, since it will take time for the plasma treated and non-plasma treated parts of the molecules to diffuse to and from the surface. The degree of unavoidable plasma induces cross-linking in the polymer will prevent the plasma-induced surface modification in disappearing completely. The element composition for the reference membrane is observed to be unchanged for a very long time. However, after somewhere between 1680 hours (70 days) and 3240 hours (135 days) the oxygen content is observed to increase slightly. This is believed to be caused by a "natural" oxidation from the ambient conditions.

Table 5 presents the distribution of carbon functionalities in the reference PPSU membrane and the low-pressure plasma treated (4 min at
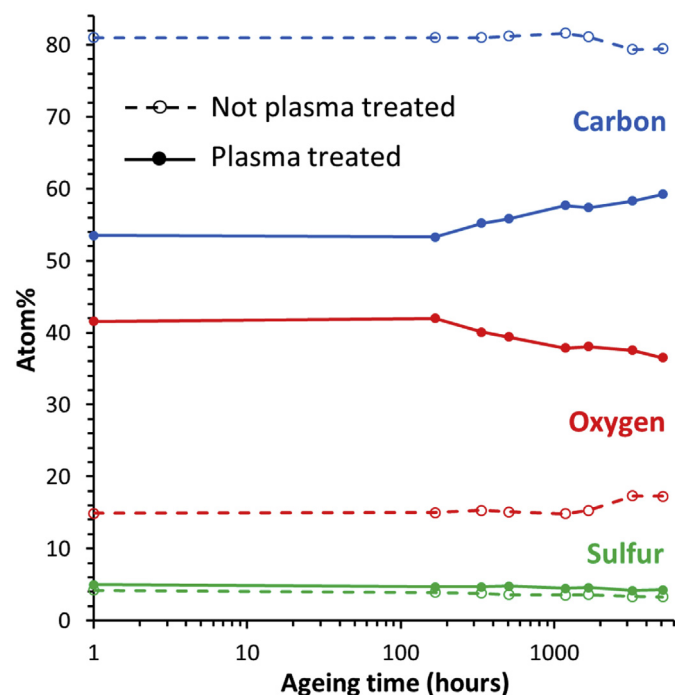
Table 5

Quantification of deconvoluted C 1s spectra for aged and non-aged PPSU membranes that are either plasma treated or not.

Peak	No plasma No ageing [%]	No plasma Aged 212 days [%]	Plasma treated[a] No ageing [%]	Plasma treated[a] Aged 212 days [%]
C=C	57.9	57.1	28.3	53.4
C–C	20.7	24.3	27.2	21.2
C–S	8.3	8.3	6.1	7.2
C–O	12.6	8.4	18.6	7.0
C=O	0.5	1.2	8.6	9.0
(C=O)–O	0.0	0.8	11.2	2.2

[a] Low-pressure plasma (5×10^{-3} Torr, 4 min).

1000 W) PPSU membrane after fabrication and after 212 days of ageing (darkness, ambient air, room temperature). From Fig. 4 it is evident that the reference sample has undergone a minor oxidation (presumably from ambient conditions) after having been stored for 212 days. However, Table 5 reveals more details of the oxidation process. The level of C–S remains the same during ageing for the reference sample, which suggests that the sulfone group is unaffected. This is supported by the S 2p XPS spectrum (not shown) for the aged reference sample. The C–O level decreases from 12.6% to 8.4% for the reference sample during ageing, suggesting that the ether group in the polymer backbone is oxidized resulting in chain scission. The minor degree of C=O and (C=O)–O formation for the reference sample during ageing can only happen in connection with a ring opening. The C 1s XPS spectra for the non-aged and aged plasma treated samples are shown in Fig. 1c and Fig. 1d, which reveal details of the ageing effect involving suspected diffusion of non-oxidized PPSU to the surface, and diffusion of oxidized PPSU to the bulk. If the diffusion theory is correct then there should be certain predicted developments in the carbon functionalities. The aromatic functionality (C=C) should increase as the surface will be enriched in non-oxidized PPSU during ageing, which is consistent with the observation, i.e. the C=C content increases from 28.3% to 53.4%. Furthermore, the C–C and C–S levels are expected to approach the reference level, which is also consistent with the observation. According to Fig. 4 the oxygen level decreases during ageing for the plasma treated sample, so it is expected that carbon-oxygen functionalities will decrease during ageing. This is indeed the observation for (C=O)–O that decreases from 11.2% to 2.2%. However, the fact that the C=O level remains unchanged and C–O decreases from 18.6% to 7.0% is a surprise. It is the most polar functionalities that are expected to diffuse into the bulk, i.e. (C=O)–O (carboxylic acids and esters) and C=O (aldehydes and ketones). The C–O functionality originates from the native ether functionality (Ar-O-Ar) that should increase during ageing (for the same reason that C=C increases). However, C–O can also originate from the plasma oxidation product Ar-O-R and R-O-R, where R represents aliphatic carbon or hydrogen, but these are not as polar as (C=O)–O and C=O, so it is a mystery why the C–O level decreases significantly. For the same reason it is surprising that the C=O level remains the same during ageing. The plasma treated PPSU sample is expected to be slightly oxidized during ageing for the same reason that the reference PPSU sample is slightly oxidized during ageing. However, this contribution is expected to be negligible compared to the diffusion phenomena observed for the aged plasma treated sample. No explanation has been found for the decrease of C–O and the unchanged level of C=O during ageing for the plasma treated PPSU sample.

The observations in this work suggest that oxidized PPSU and possible fragments of PPSU diffuse into the bulk and non-oxidized PPSU diffuse out to the surface. This is an unfortunate phenomenon since the oxidized PPSU contains the desired properties (i.e. increased wettability), so it is relevant from a practical point of view to determine the time scale for the disappearing of the desired surface properties. The plasma-induced cross-linking will partly prevent diffusion, however, the degree of cross-linking is not known in this case. In order to evaluate the

Fig. 4. Plots of the element compositions for a PPSU membrane that was plasma treated (solid lines, 1000 W, 4 min), and a PPSU membrane that was not plasma treated (dashed lines) as a function of time in darkness at room temperature in ambient air. The experiment was stopped after 5088 hours (212 days). Each point is an average based on five measurements on different surface locations.

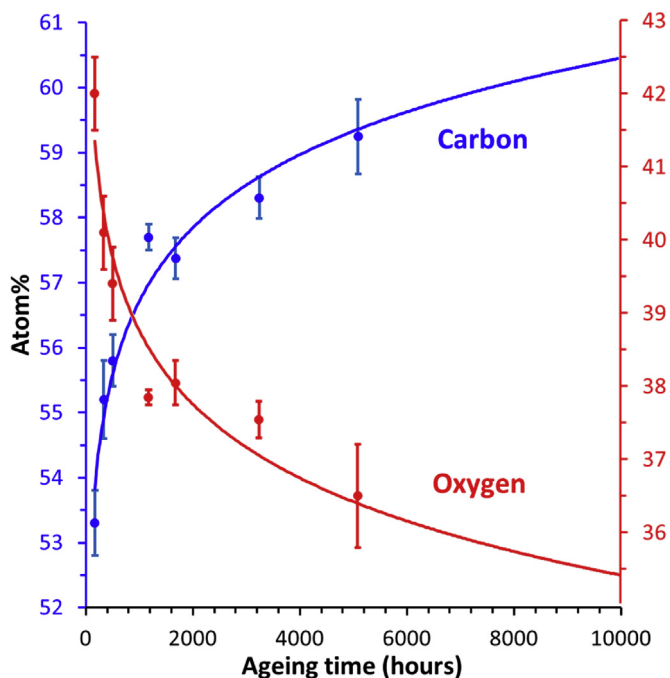**Fig. 5.** A plot of the carbon and oxygen contents for a PPSU membrane that was plasma treated (1000 W, 4 min) as a function of time in darkness at room temperature in ambient air. The experiment was stopped after 5088 hours (212 days). The plots are extrapolated to 10000 hours (417 days). Each point is an average based on five measurements on different surface locations.

time scale for the disappearing of the surface properties the carbon and oxygen content versus time was fitted to a curve and extrapolated to 10000 hours (417 days). The result is presented in Fig. 5. The plots exhibit a logarithmic behavior typical for diffusion processes. According to Fig. 5 the carbon and oxygen content will only change by ~1 atom% from the 212 days where the experiment was stopped to 417 days. If the plots are extrapolated to values corresponding to the values found in the reference sample, then it will take several hundreds of thousands of

years, so for all practical purposes the surface properties will never completely disappear within the expected lifetime of a membrane in operation. It can thus be concluded that the plasma-induced surface properties will diminish in time but for all practical purposes not vanish. However, in some cases the nanofibrous membranes are coated with another material providing specific properties, e.g. nanofibrous PPSU membranes have been coated with Aquaporin [34], which is hydrophilic and thus requires a hydrophilic PPSU surface. Aquaporin is a water channel protein that provides selective conduits for water with a high osmotic permeability [45, 46]. If a hydrophilic material is coated onto the PPSU fiber surface, such as for example Aquaporin, then it is likely that the coated hydrophilic material will prevent or partly prevent the diffusion of oxidated PPSU, i.e. the hydrophilic oxidated PPSU is locked on the fiber surface from interactions with the hydrophilic Aquaporin. No attempts have been made to study this possible phenomenon since the coating prevents XPS analysis of the buried PPSU surface.

3.3. Wettability

As previously discussed the wettability is controlled by the plasma-induced formation of hydrophilic carbon functionalities on the PPSU surface. The degree of wettability can be evaluated from a contact angle analysis, i.e. the lower the contact angle the greater the wettability. The contact angle for the hydrophobic reference sample was measured to 129.7° consistent with a hydrophobic surface. It was not possible to measure the contact angles for the PPSU samples that were low-pressure plasma treated. The droplets were efficiently sucked into the nanofibrous network, which suggests that all the surfaces in question presumably have an extremely high degree of wettability. However, it should be emphasized that porosity could contribute to the disappearing phenomenon of the droplets.

With respect to the atmospheric-pressure plasma treated samples it was possible to measure contact angles, which suggests some degree of hydrophilicity. However, due to an apparent significant random variation of the measured contact angles, ranging from 65° and 90° (average of three measurements on each sample) for all exposure times, it suggests that an inhomogeneity is in play, so the question is what the origin of this inhomogeneity is. Fig. 6 presents (i) the carbon and oxygen contents, and (ii) the fraction of C=O and (C=O)–O relative to all carbon, for PPSU
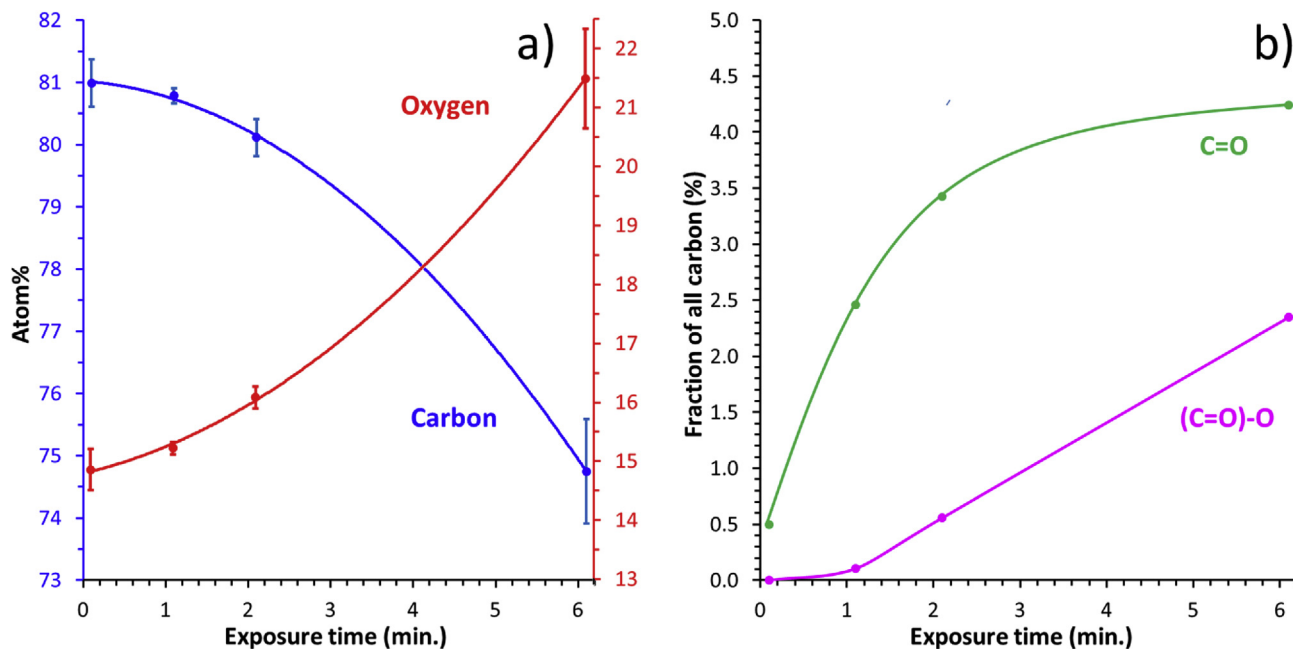
Fig. 6. XPS results for PPSU membranes that were atmospheric-pressure plasma treated as a function of exposure time. (a) Carbon and oxygen contents. Each point is an average based on five measurements on different surface locations. (b) Fraction of C=O and (C=O)–O relative to all carbon (single measurements).

membranes that were atmospheric-pressure plasma treated as a function of exposure time. As is evident there is a non-random correlation between exposure time and (i) the oxygen content, and (ii) fraction of C=O and (C=O)–O relative to all carbon, suggesting that the plasma treatment results in a well-controlled homogeneous oxidation, i.e. non-random. The apparent significant random variation of the measured contact angles for the atmospheric-pressure plasma treated samples must thus originate from somewhere else. A possible source could be inhomogeneities in the surface treatment. For example, the membrane is not completely flat and mild heating during the plasma treatment can further promote deformations that affect the distance between the membrane surface and the coplanar barrier discharge (2.5 mm gap). Moreover, the discharge is not completely uniform as can be seen from Fig. 1 in ref [41].

4. Conclusion

The electrospun PPSU nanofibrous membrane is a promising candidate for water purification applications. In this work PPSU membranes were systematically subjected to low-pressure or atmospheric-pressure plasma treatment in order to control the surface chemistry, which is important for controlling the necessary hydrophilicity and thereby the wettability of the membrane surfaces. The atmospheric-pressure plasma exhibits a limited controllability but compliments the more flexible low-pressure plasma since the atmospheric-pressure plasma represents subtle plasma treatment (under the conditions in question) that is more difficult to control with low-pressure plasma. Low-pressure plasma readily produces polar chemical anchor groups such as (C=O)–O and C=O that are important for hydrophilicity, but variation was difficult to achieve unless complementary atmospheric-pressure plasma is considered that produces a smaller degree of (C=O)–O and C=O. The atmospheric-pressure plasma provided hydrophilicity/wettability that made it possible to measure a contact angle, but for all the low-pressure plasma conditions the droplets was sucked into the PPSU membranes, which suggests a very high degree of wettability. Monitoring temporal developments of element compositions for a reference membrane and a low-pressure plasma treated membrane revealed age effects. The reference membrane exhibited a minor degree of oxidation presumably from ambient air. The low-pressure plasma treated membrane changed significantly over a period of 212 days that was assigned to a diffusion phenomenon where oxidated PPSU diffuse into the non-oxidated PPSU bulk, and the non-oxidated PPSU from the bulk diffuse out to the surface. It was shown that the improved hydrophilicity/wettability will diminish but not vanish in time.

Data availability

The raw/processed data required to reproduce these findings cannot be shared at this time due to technical or time limitations.

Declarations

Author contribution statement

Kion Norrman: Conceived and designed the experiments; Performed the experiments; Analyzed and interpreted the data; Contributed reagents, materials, analysis tools or data; Wrote the paper.

Eugen Stamate: Conceived and designed the experiments; Performed the experiments.

Wenjing Zhang, Yan Wang: Contributed reagents, materials, analysis tools or data.

Funding statement

Competing interest statement

The authors declare no conflict of interest.

Additional information

No additional information is available for this paper.

Acknowledgements

References

[1] J. Xue, J. Xie, W. Liu, Y. Xia, Electrospun nanofibers: new concepts, materials, and applications, Acc. Chem. Res. 50 (2017) 1976–1987.

[2] D.I. Braghirolli, D. Steffens, P. Pranke, Electrospinning for regenerative medicine: a review of the main topics, Drug Discov. Today 19 (2014) 743–753.

[3] M. Kitsara, O. Agbulut, D. Kontziampasis, Y. Chen, P. Menasché, Fibers for hearts: a critical review on electrospinning for cardiac tissue engineering, Acta Biomater. 48 (2017) 20–40.

[4] Z.M. Huang, Y. Zhang, Z. Kotaki, S. Ramakrishna, A review on polymer nanofibers by electrospinning and their applications in nanocomposites, Compos. Sci. Technol. 63 (2003) 2223–2253.

[5] X. Shi, W. Zhou, D. Ma, Q. Ma, D. Bridges, Y. Ma, A. Hu, Electrospinning of nanofibers and their applications for energy devices, J. Nanomater. 2015 (2015) 1–20.

[6] M. Mirjalili, S. Zohoori, Review for application of electrospinning and electrospun nanofibers technology in textile industry, J. Nanostruct. Chem. 6 (2016) 207–213.

[7] S.S. Ray, S.-S. Chen, C.-W. Li, N.C. Nguyen, H.T. Nguyen, A comprehensive review: electrospinning technique for fabrication and surface modification of membranes for water treatment application, RSC Adv. 6 (2016) 85495–85514.

[8] F.E. Ahmed, B. S Lalia, R. Hashaikeh, A review on electrospinning for membrane fabrication: challenges and applications, Desalination 356 (2015) 15–30.

[9] P.S. Suja, C.R. Reshmi, P. Sagitha, A. Sujith, Electrospun nanofibrous membranes for water purification, Polym. Rev. 57 (2017) 467–504.

[10] B. Satilmis, P.M. Budd, Tamer Uyar, Systematic hydrolysis of PIM-1 and electrospinning of hydrolyzed PIM-1 ultrafine fibers for an efficient removal of dye from water, React. Funct. Polym. 121 (2017) 67–75.

[11] G. Ren, X. Xu, Q. Liu, J. Cheng, X. Yuan, L. Wu, Y. Wan, Electrospun poly(vinyl alcohol)/glucose oxidase biocomposite membranes for biosensor applications, React. Funct. Polym. 66 (2006) 1559–1564.

[12] A. Senecal, J. Magnone, P. Marek, K. Senecal, Development of functional nanofibrous membrane assemblies towards biological sensing, React. Funct. Polym. 68 (2008) 1429–1434.

[13] J. Quirós, A.J.R. Amaral, G. Pasparakis, G.R. Williams, R. Rosal, Electrospun boronic acid-containing polymer membranes as fluorescent sensors for bacteria detection, React. Funct. Polym. 121 (2017) 23–31.

[14] D. Simões, S.P. Miguel, I.J. Correia, Biofunctionalization of electrospun poly(caprolactone) fibers with Maillard reaction products for wound dressing applications, React. Funct. Polym. 131 (2018) 191–202.

[15] R. Morsy, M. Hosny, F. Reicha, T. Elnimr, Developing a potential antibacterial long-term degradable electrospun gelatin-based composites mats for wound dressing applications, React. Funct. Polym. 114 (2017) 8–12.

[16] P. Raghavan, D.-H. Lim, J.-H. Ahn, C. Nah, D.C. Sherrington, H.-S. Ryu, H.-J. Ahn, Electrospun polymer nanofibers: the booming cutting edge technology, React. Funct. Polym. 72 (2012) 915–930.

[17] R. Asmatulu, H. Muppalla, Z. Veisi, W.S. Khan, A. Asaduzzaman, N. Nuraje, Study of hydrophilic electrospun nanofiber membranes for filtration of micro and nanosize suspended particles, Membranes (Basel) 3 (2013) 375–388.

[18] K. Yoon, B.S. Hsiao, B. Chu, Formation of functional polyethersulfone electrospun membrane for water purification by mixed solvent and oxidation processes, Polymer 50 (2009) 2893–2899.

[19] M. Botes, T.E. Cloete, The potential of nanofibers and nanobiocides in water purification, Crit. Rev. Microbiol. 36 (2010) 68–81.

[20] Y. Tian, M. Wu, R. Liu, Y. Li, D. Wang, J. Tan, R. Wu, Y. Huang, Electrospun membrane of cellulose acetate for heavy metal ion adsorption in water treatment, Carbohydr. Polym. 83 (2011) 743–748.

[21] Z. Ma, M. Kotaki, S. Ramakrishna, Surface modified nonwoven polysulphone (PSU) fiber mesh by electrospinning: a novel affinity membrane, J. Membr. Sci. 272 (2006) 179–187.

[22] R. Gopal, S. Kaur, Z. Ma, C. Chan, S. Ramakrishna, T. Matsuura, Electrospun nanofibrous filtration membrane, J. Membr. Sci. 281 (2006) 581–586.

[23] S.S. Choi, S.G. Lee, C.W. Joo, S.S. Im, S.H. Kim, Formation of interfiber bonding in electrospun poly(etherimide) nanofiber web, J. Mater. Sci. 39 (2004) 1511–1513.

[24] Z.W. Ma, M. Kotaki, S. Ramakrishna, Electrospun cellulose nanofiber as affinity membrane, J. Membr. Sci. 265 (2005) 115–123.

[25] M. Hayama, K. Yamamoto, F. Kohori, T. Uesaka, Y. Ueno, H. Sugaya, I. Itagaki, K. Sakai, Nanoscopic behavior of polyvinylpyrrolidone particles on polysulfone/polyvinylpyrrolidone film, Biomaterials 25 (2004) 1019–1028.

[26] S. Sun, Y. Yue, X. Huang, D. Meng, Protein adsorption on blood-contact membranes, J. Membr. Sci. 222 (2003) 3–18.

[27] A. Hamza, V.A. Pham, T. Matsuura, J.P. Santerre, Development of membranes with low surface energy to reduce the fouling in ultrafiltration applications, J. Membr. Sci. 131 (1997) 217–227.

[28] C.H. Bamford, K.G. Al-Lamee, Studies in polymer surface modification and grafting for biomedical uses. 2. application to arterial blood filters and oxygenators, Polymer 37 (1996) 4885–4889.

[29] F.S. Denes, S. Manolache, Macromolecular plasma-chemistry: an emerging field of polymer science, Prog. Polym. Sci. 29 (2004) 815–885.

[30] J. Feng, G. Wen, W. Huang, E. Kang, K.G. Neoh, Influence of oxygen plasma treatment on poly(ether sulphone) films, Polym. Degrad. Stabil. 91 (2006) 12–20.

[31] T. Vrlinic, A. Vesel, U. Cvelbar, M. Krajnc, M. Mozetic, Rapid surface functionalization of poly(ethersulphone) foils using a highly reactive oxygen-plasma treatment, Surf. Interface Anal. 39 (2007) 476–481.

[32] D.S. Wavhal, E.R. Fisher, Hydrophilic modification of polyethersulfone membranes by low temperature plasma-induced graft polymerization, J. Membr. Sci. 209 (2002) 255–269.

[33] E. Gonzalez, M.D. Barankin, P.C. Guschl, R.F. Hicks, Ring opening of aromatic polymers by remote atmospheric-pressure plasma, IEEE Trans. Plasma Sci. 37 (2009) 823–831.

[34] Y. Wang, R. Górecki, E. Stamate, K. Norrman, D. Aili, M. Zuo, W. Guo, C. Hélix-Nielsen, W. Zhang, Preparation of super-hydrophilic polyphenylsulfone nanofiber membranes for water treatment, RSC Adv. 9 (2019) 278–286.

[35] L. Bardos, H. Barankova, Cold atmospheric plasma: sources, processes, and applications, Thin Solid Films 518 (2010) 6705–6713.

[36] D. Pappas, Status and potential of atmospheric plasma processing of materials, J. Vac. Sci. Technol. A 29 (2011), 020801-1-17.

[37] A. Lacoste1, T. Lagarde, S. Béchu1, Y. Arnall, J. Pelletier, Multi-dipolar plasmas for uniform processing: physics, design and performance, Plasma Sources Sci. Technol. 11 (2002) 407–412.

[38] E. Stamate, M. Draghici, High electronegativity multi-dipolar electron cyclotron resonance plasma source for etching by negative ions, J. Appl. Phys. 111 (2012), 083303-1–6.

[39] E. Stamate, Status and challenges in electrical diagnostics of processing plasmas, Sur. Coat. Technol. 260 (2014) 401–410.

[40] M. Simor, J. Rahel, P. Vojtek, M. Cernak, A. Brablec, Atmospheric-pressure diffuse coplanar surface discharge for surface treatments, Appl. Phys. Lett. 81 (2002) 2716–2718.

[41] I. Jõgi, K. Erme, E. Levoll, E. Stamate, Radical production efficiency and electrical characteristics of a coplanar barrier discharge built by multilayer ceramic technology, J. Phys. D: Appl. Phys. 50 (2017) 465201.

[42] A.V. Naumkin, A. Kraut-Vass, S.W. Gaarenstroom, C.J. Powell, NIST Standard Reference Database 20, version 4.1, web version, 2012. accessed, http://srdata.nist.gov/xps/. (Accessed February 2018).

[43] K. Norrman, P. Kingshott, B. Kaeselev, A. Ghanbari-Siahkali, Photodegradation of poly(ether sulphone). Part 1. A time-of-flight secondary ion mass spectrometry study, Surf. Interface Anal. 36 (2004) 1533–1541.

[44] K. Norrman, F.C. Krebs, Photodegradation of poly(ether sulphone). Part 2. Wavelength and atmosphere dependence, Surf. Interface Anal. 36 (2004) 1542–1549.

[45] C. Tang, Z. Wang, I. Petrinić, A.G. Fane, C. Hélix-Nielsen, Biomimetic aquaporin membranes coming of age, Desalination 368 (2015) 89–105.

[46] A. Giwa, S.W. Hasan, A. Yousuf, S. Chakraborty, D.J. Johnson, N. Hilal, Biomimetic membranes: a critical review of recent progress, Desalination 420 (2017) 403–424.